

Level-crossing determination of the $6s6p\ ^3P_1$ hfs of ^{193m}Hg †

O. Redi and H. H. Stroke

Department of Physics, New York University, New York, New York 10003

(Received 12 November 1973)

The magnetic-dipole and electric-quadrupole hfs interaction constants of 11-h ^{193m}Hg in the $6s6p\ ^3P_1$ state were determined from the observation of four level crossings. Previous studies relied on the observation of a single level crossing (W. W. Smith) and on optical spectroscopic data. The results, with second-order hyperfine, Zeeman, and cross Zeeman-hyperfine corrections are $A = -2399.60(3)$ MHz and $B = -655.6(18)$ MHz. The calculated hfs anomaly $^{193m}\Delta^{199}$ is 1.055(1)%, and the resulting electric-quadrupole moment is 1.2(1) b. The isotope shift is redetermined by the new hfs results.

I. INTRODUCTION

As part of our continuing investigation¹⁻³ of the systematics of the nuclear structure of heavy elements through its influence on the atomic spectrum, we have measured, with the use of the level-crossing technique, the hyperfine structure (hfs) of the $(6s6p)\ ^3P_1$ state of 11-h ^{193m}Hg . Previously this hfs was studied by optical spectroscopy^{1,4} as well as by the level-crossing technique,⁵ but the earlier study was incomplete in that only the "main" level crossing (defined in Fig. 2) was detected and measured. ^{193m}Hg has a nuclear spin $I = \frac{13}{2}$, and therefore the 3P_1 hfs involves both a magnetic-dipole and an electric-quadrupole interaction. Therefore, with this single level-crossing measurement the determination of the hfs constants could be made only with the additional use of the optical spectroscopic data. The accuracy of these data that yielded the electric-quadrupole interaction constant B , however, is largely limited by the Doppler width of the spectral lines. The value of the magnetic-dipole hfs interaction constant A depends only slightly on the spectroscopic data, and its accuracy is affected by the natural linewidth. In the present work we report the measurement of two additional level crossings for this isotope. These "foldover" crossings are labeled 3 and 4 in Fig. 2. The new data yield a somewhat improved value of A and a much more accurate one of B . If we combine the recent direct measurements^{3,6} of the nuclear magnetic moment with the hfs data, the hfs anomaly can be determined. The hfs anomaly,⁷ or Bohr-Weisskopf effect, reflects the influence of the distributed nuclear magnetization on the hfs. Our new data are also used to calculate improved values of the quadrupole moment and the isotope shift, and serve to check the spin assignment.

II. EXPERIMENT

A. Level-crossing method

Our experiment was made with the use of the level-crossing technique.^{8,9} In this, the variation of the angular distribution of the $(6s6p)\ ^3P_1$ - $(6s^2)\ ^1S_0$ 2537-Å resonance radiation, scattered by ^{193m}Hg atoms in a cell, is monitored as a function of an externally applied magnetic field in the vicinity of the value for which two 3P_1 substates, μ and μ' , with energies E_μ and $E_{\mu'}$, become degenerate (level crossing). Here the intensity I of the scattered light is given by

$$I \propto R_0 + \frac{A_{\mu\mu'} + A_{\mu\mu'}^*}{1 + x^2} - \frac{ix(A_{\mu\mu'} - A_{\mu\mu'}^*)}{1 + x^2} \quad (1)$$

where $x \equiv \tau(E_\mu - E_{\mu'})/\hbar$, τ is the excited-state mean life, and R_0 represents scattered light that is independent of x . $A_{\mu\mu'}$, defined and calculated in Ref. 2, depends on matrix elements of the electric-dipole operator and the geometry involved in the scattering process. Our experiment was adjusted to have the incident and scattered light and the applied magnetic field mutually perpendicular. If this condition is achieved, $A_{\mu\mu'}$ is real and hence the term in (1), which has a dispersion-like shape, is zero. Furthermore, with this arrangement $A_{\mu\mu'}$ is nonzero only for $|\mu - \mu'| = 2$.

The energy levels of the 3P_1 hfs of ^{193m}Hg in an external magnetic field are shown in Fig. 1. An enlargement of the region in which the level crossings were observed is shown in Fig. 2. The measurements of the fields at which the crossings occur, together with the other requisite data given in Sec. III B, allow the determination of A and B . The uniqueness of this determination is discussed in Sec. III A.

B. Apparatus

The experimental arrangement is shown in Fig. 3. The apparatus was identical to that described by us in detail in Ref. 2, except for the fact that the lamp contained high isotopic purity ^{198}Hg (>99%) and that a different type of magnet was used to vary the wavelength through the value necessary to excite the ^{193}Hg levels which are crossing. We used the σ light emitted perpendicularly to the magnetic field, and eliminated the π Zeeman component, unshifted by the field, with the use of a linear polarizer.¹⁰

C. Procedure and results

The ^{193}Hg was produced by a $^{197}\text{Au}(\rho, 5n)$ reaction¹¹ with the use of 55-MeV protons from the Harvard University cyclotron. The 0.15-mm-thick gold foil was bombarded internally with a 1- μA beam for 12 h, producing $\sim 10^{14}$ atoms. The vacuum system and the procedure for transferring the radioactive mercury from the target into the scattering cell are described in Ref. 12. The cubic scattering cell, 1 cm on a side, was made from a commercial unit,¹³ as described in Ref. 2. This cell was used in the experiment at room temperature.¹⁴

In experiments with short-lived radioactive isotopes, the time-consuming search for level-crossing magnetic fields can be an important limitation on the amount of data obtainable. This

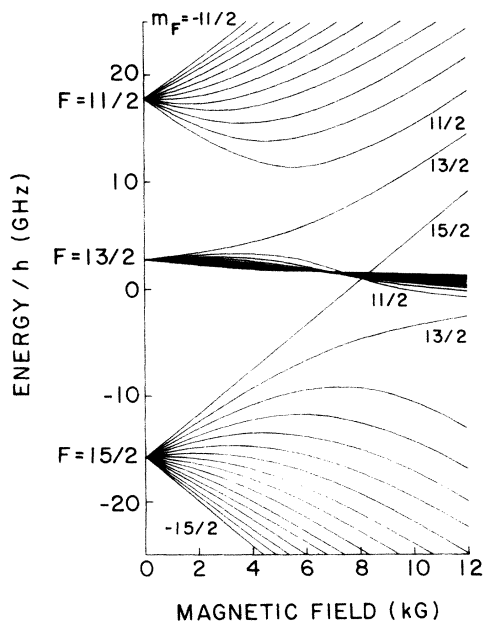


FIG. 1. Magnetic field dependence of hfs energy levels of ^{193}mHg in the $6s6p\ ^3P_1$ state.

problem was greatly reduced in this experiment by making use of the previously available ^{193}mHg hfs and isotope-shift data to narrow the magnetic field search range of the level crossings to a few hundred gauss and to determine the corresponding magnetic field shift needed for the lamp.

For the measured level crossings (Nos. 3 and 4, Fig. 2), we calculate¹⁵ changes of intensity at the photomultiplier ranging from 2 to 3%. Since there are present in the cell other isotopes of mercury produced by the nuclear reactions, the value of R_0 will be greater than that for ^{193}mHg alone. Therefore the above calculation gives an upper limit on the actual intensity change. In order to observe such level-crossing signals with a good signal-to-noise ratio, a lock-in detection system with magnetic field modulation was used.

Four level crossings were observed in the magnetic field region of 7.3–8.1 kG with a lamp scanning field of 6.0 kG. The identification of these level crossings with ^{193}mHg and specifically with the $\Delta m_F = 2$ crossings Nos. 1–4 in Fig. 2 is discussed in Sec. III. Precision measurements were made for level crossings Nos. 1, 3, and 4. The results of these measurements are given in Table I. An

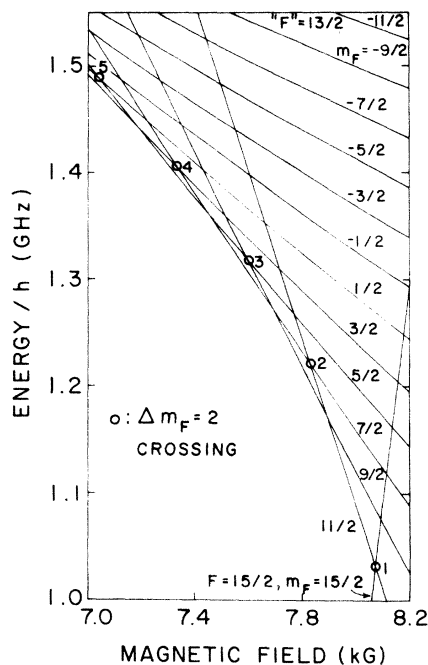


FIG. 2. Details of the ^{193}mHg hyperfine energy-level diagram (Fig. 1) in the region of the $\Delta m_F = 2$ level crossings studied in this work. The "main" crossing (i.e., of m_F levels originating from different zero-field states) and the "foldover" crossings are labeled No. 1 and Nos. 2–5, respectively. (Only four of the eleven $\Delta m_F = 2$ foldover crossings can be seen in this diagram.)

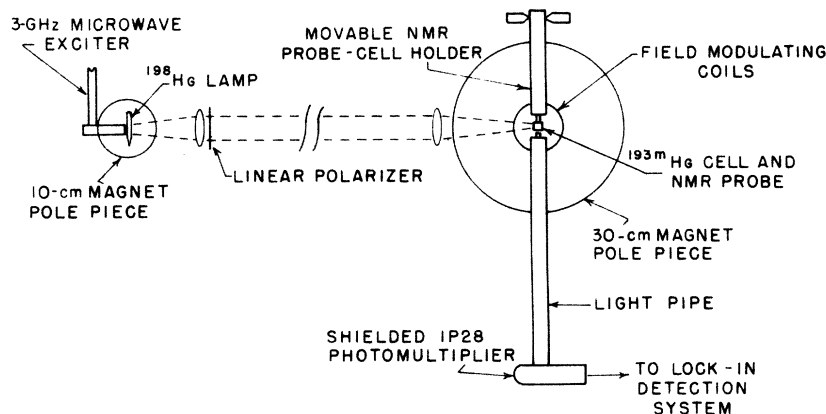


FIG. 3. Schematic diagram of the apparatus. The lock-in detection system consists of a Princeton Applied Research JB-5 lock-in amplifier, an audio amplifier for driving the magnetic-field modulation coils, and a strip-chart recorder. The movable NMR probe-cell holder allowed a quick interchange of the probe and the cell to permit a cell-to-probe field correction measurement.

approximate value of the magnetic field of level crossing No. 2 was determined to be 7835(50) G. This rough determination served as a further consistency check on the interpretation of all the data. Figures 4(a) and 4(b) show typical recorder traces of the lock-in detector output versus magnetic fields for level crossings Nos. 3 and 4. The large slope of the baseline seen in Fig. 4(b) is due to a change in "modulation pickup." Modulation pickup arises from the Zeeman modulation of the wavelength of the absorption lines of the atoms in the cell, relative to the fixed spectrum of the incident light.

The Lorentzian linewidths calculated¹⁶ from the lock-in detector output curves were found to be 20(4) and 27(5) G for level crossings Nos. 3 and 4. The corresponding widths ΔH , calculated from

$$\Delta H = \left| \frac{dH}{d(E_\mu - E_{\mu'})} \right| \frac{2\hbar}{\tau},$$

with¹⁷ $\tau = 1.18(2) \times 10^{-7}$ sec, are 13 and 21 G, in disagreement with the experimental values. We assume this disagreement to result from residual gas-pressure broadening. It has been shown experimentally¹⁸ that, to a precision of better than one part in 10^6 , there are no displacements of the crossing field either under the influence of mercury-mercury or mercury-foreign-gas collisions, up to pressures of several Torr, or because of trapping of resonance radiation. Other possible systematic errors were investigated previously.²

TABLE I. ¹⁹³Hg level-crossing magnetic field data^a given as NMR frequencies ν_p . The magnetic field measurements were made with a proton NMR probe^b for which the product of the Bohr magneton in frequency units, μ_B/h , and the magnetic field H are related to ν_p by $\mu_B H/h = 328.7323(3)\nu_p$. The NMR probe-scattering cell magnetic field difference, typically 50 mG, was measured by interchanging the NMR probe and cell position. The identification of crossing sublevels m_F and m'_F is discussed in Sec. III.

Crossing no.	(m_F, m'_F)	ν_p (kHz)	Weighted mean of all data (kHz)
1	$(\frac{15}{2}, \frac{11}{2})$	34 381.24(50)	
1		34 380.51(42) ^c	
1			34 380.81(33)
3	$(\frac{9}{2}, \frac{5}{2})$	32 372(8) ^d	32 372(8)
4	$(\frac{7}{2}, \frac{3}{2})$	31 231(10)	31 231(10)

^a Preliminary results were presented in Bull. Am. Phys. Soc. **10**, 456 (1965).

^b See Ref. 2.

^c This value is from Ref. 5.

^d This result has been corrected for deviation from perfect antisymmetry of the lock-in detector output curve. The correction [a subtraction of 5(2) kHz from the raw data] was made with the use of Eq. (A9) of Ref. 5, which is sufficiently accurate for the low magnetic field modulation used.

III. ANALYSIS AND DISCUSSION

A. Identification of observed level crossings

We attribute the observed signals to $^{193m}\text{Hg } \Delta m_F = 2$ level crossings for the following reasons:

(i) The experiment has a very specific sensitivity to mercury because of the requirement of an overlap of a mercury emission line with an absorption line of the atoms in the cell, and because of the requirement of sufficient vapor pressure at room temperature.

(ii) Only $\Delta m_F = 2$ level crossings are observable with the rectangular geometry used in this experiment (see Ref. 2).

(iii) All level crossings associated with isotopes and isomers of mercury, except ^{193}Hg and ^{193m}Hg , produced by the 55-MeV $\text{Au}(\beta, xn)$ reactions have experimentally well known or precisely calculable magnetic field values. On this basis the observed level crossings can be assigned only to ^{193}Hg or ^{193m}Hg or both.

(iv) Earlier results for the ^{193}Hg ($I = \frac{3}{2}$) hfs and magnetic-moment measurements imply that at most one $\Delta m_F = 2$ level crossing is expected for this isotope in the magnetic field region of the

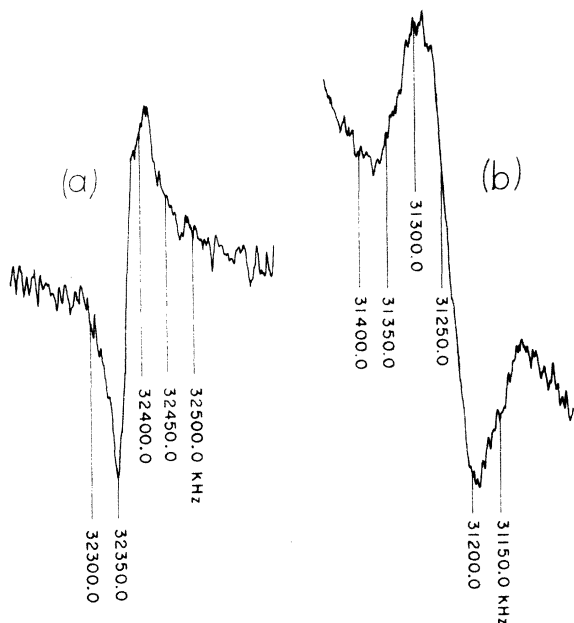


FIG. 4. Typical recorder tracings of the lock-in detector output, obtained with a 3-sec time constant, for (a) level crossing No. 3, and (b) level crossing No. 4. The NMR frequency markers define the magnetic field scale. Results from increasing and decreasing magnetic field sweeps (rate = 12 G/min) were averaged in order to cancel the shifts due to response lag time of the lock-in detector.

signals reported here.

(v) A satisfactory fit of the four measured level-crossing field values can be obtained with a hyperfine Hamiltonian for $I = \frac{13}{2}$ —the known spin of ^{193m}Hg .

Uniqueness of the hyperfine-structure determination from the level-crossing magnetic field values was investigated. The nuclear spin and the 3P_1 state A value (obtained, within the hfs anomaly, from the optical-pumping data^{3,6}) are known for ^{193m}Hg . Hence it is sufficient to check the uniqueness of the determination of B . This was done with the use of the graphs shown in Figs. 5 and 6, as well as a graph covering a larger range of B/A . The graphs indicated that, considering all B/A values, there is at least rough agreement between the set of predicted and experimental level-crossing magnetic fields only for $0 \lesssim B/A \lesssim \frac{1}{2}$. Only one B/A value in this range gave consistency between experimental and exactly calculated values. The other possibilities in this range, suggested by the graphs but found to be inconsistent with the data, arise only if we consider (a) the unlikely possibility of the existence of one more ^{193m}Hg level crossing than was detected in this experiment in the field range of 7.3–8.1 kG, and (b) the possibility, suggested by our recent work,¹⁹ that a $\Delta m_F = 2$ ^{193}Hg level crossing may exist in the above magnetic field range²⁰ and thus could be mistaken for a ^{193m}Hg level crossing. The energy-level diagram in a magnetic field, showing the unique assignment of quantum numbers to the observed level crossings, is shown in Figs. 1 and 2.

As discussed in Ref. 2, the level-crossing data alone are not usually sufficient to allow a unique determination of the nuclear spin and/or the sign of the interaction constants (only the sign of B/A is determined).

Since, in this case, we have other than level-crossing data, no such ambiguity exists for ^{193m}Hg . Indeed, when our level-crossing results are combined with the optical-spectroscopic^{1,4} and the optical-pumping^{3,6} data, we obtain further verification of the value of the nuclear spin $I = \frac{13}{2}$.

B. Calculation of hfs

The hyperfine and Zeeman interactions mix the $(6s6p)^3P_2$, 3P_1 , 3P_0 , and 1P_1 atomic states sufficiently to give rise to shifts of the 3P_1 level-crossing field values: In the present instance these are typically four times the experimental uncertainty of the field values. The magnitude and sign of these shifts are such that a satisfactory fit ($\chi^2 = 0.4$) can be obtained, by least-squares minimization, between the experimental and theoretical

level-crossing field values even when the latter are calculated without taking this mixing into account. Such a calculation, carried out with the use of the HYPERFINE 4-A computer program,²¹ yields the uncorrected hyperfine interaction constants A' and B' given in Table IV. These are used in the calculation of the corrected hfs interaction constants, as described below. The uncorrected constants are specific to the magnetic

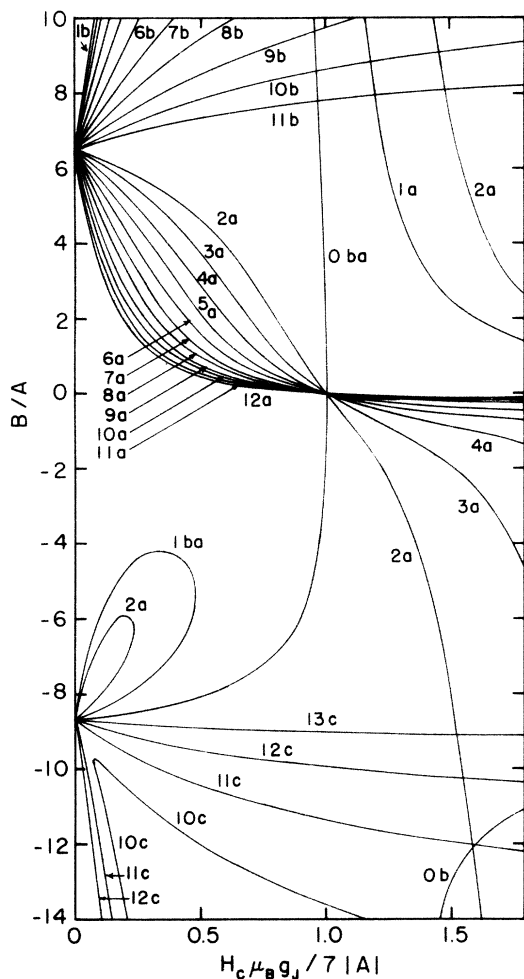


FIG. 5. Relationship, for $I = \frac{13}{2}$, $J = 1$, between B/A and the level-crossing magnetic-field values H_c , given in units of $7|A|/\mu_B g_J$. The crossing levels are labeled by their m_F (indicated by numbers n) and high-field m_J (indicated by letters a, b, c) quantum numbers. The correspondence of the value of n with the m_F levels is given by $m_F = \frac{13}{2} - n$ and $m'_F = \frac{11}{2} - n$. For the letters we identify a with $m_J = m'_J = 0$, b with $m_J = m'_J = +1$, and c with $m_J = m'_J = -1$. The two curves labeled ba have $m_J = +1$ and $m'_J = 0$. The labeling in this diagram corresponds to negative A . For positive A , the signs of all quantum numbers must be changed. The method of calculation is given in Ref. 2. The loops that are apparent here do not occur for $I < 4$.

field range and the magnetic sublevels involved in this experiment. Therefore they do not provide a basis either for comparing directly the results of different hfs measurements or for the determinations of the hfs anomaly. For this reason, and for possible other applications requiring high precision, we calculated the constants A and B corrected for the perturbations by the neighboring atomic states. These corrected constants are given by products of atomic and nuclear diagonal matrix elements, as is usually done for an isolated atomic state.

The energies of the 3P_1 hyperfine substates with second-order Zeeman, hyperfine, and cross Zeeman-hyperfine corrections were calculated using the theoretical results of Lurio, Mandel, and Novick.²² The least-squares minimization procedure for fitting hyperfine constants to the data was carried out with the HYPERFINE computer program, which was modified²³ to calculate corrected eigenvalues.

The known atomic constants for the Hg $6s6p$ configuration and the ^{199}Hg hyperfine interaction constants used in the $^{193\text{m}}\text{Hg}$ hyperfine-structure calculation are given in Table II. These constants are defined in Ref. 22.

The constant A' for $^{193\text{m}}\text{Hg}$ was used to calculate approximate values of the single-electron hyperfine interaction constants $a_s(193m)$, $a_{1/2}(193m)$, and $a_{3/2}(193m)$, from the ^{199}Hg constants given in Table II. B' was used to obtain $b_{3/2}(193m)$ with the use of Eq. (13) of Ref. 22. As a first approximation, proportionality between the single-elec-

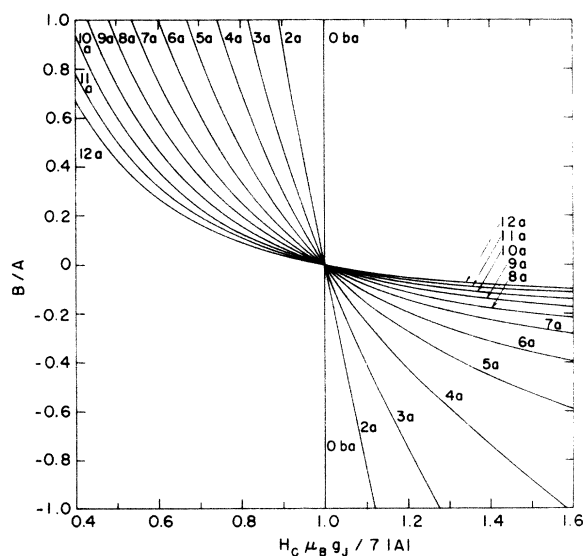


FIG. 6. Details of the graph (Fig. 5) of B/A vs level-crossing magnetic field values for $|B/A| \leq 1$.

TABLE II. Hg 6s6p configuration atomic constants^a and the ¹⁹⁹Hg hyperfine interaction constants^a used in the ¹⁹³mHg hfs calculation.

g_J	1.486 110(9) ^b
c_1	0.4278(22)
c_2	0.9038(11)
α	0.9850(4)
β	-0.1725(24)
ξ	1.094
η	1.354
δ_0	0.5298×10^8 MHz
δ_1	4.3939×10^8 MHz
δ_2	1.3882×10^8 MHz
$A(199)$	14 754.17(4) ^c MHz
$a_s(199)$	34 955(45) MHz
$a_{1/2}(199)$	5036(173) MHz
$a_{3/2}(199)$	437(15) MHz

^a See Ref. 2.

^b Level-crossing result obtained using the same apparatus as in this experiment.

^c C. V. Stager, Phys. Rev. **132**, 275 (1963); second-order corrections recalculated using the constants of this table.

tron magnetic-dipole interaction constants and the A values was assumed. Improved values, given in Table III, obtained by iteration and taking into account the hfs anomaly, did not result in values of A and B significantly different from those obtained with the approximate single-electron constants. The result of the calculation of A and B is given in Table IV. The value of A is used to calculate the hfs anomaly defined in the caption of Table III, and B is used to obtain a value of the nuclear electric-quadrupole moment Q . The calculated zero-field hyperfine separations $\Delta\nu_{15/2-11/2}$ and $\Delta\nu_{13/2-11/2}$ include the perturbations (≈ 5 MHz) by other atomic states of the 6s6p configuration.

TABLE III. ¹⁹³mHg single-electron hyperfine interaction constants. These were calculated with the relation $a_i(193m) = a_i(199)[g_I(193m)/g_I(199)](1 + {}^{193}m\Delta_i^{199})$, where $i = s, \frac{1}{2},$ or $\frac{3}{2}$ (see Table II), the ratio of the nuclear g factors, g_I , is given in the caption of Table IV, and ${}^{193}m\Delta_i^{199}$ is the single-electron hfs anomaly. The single-electron anomalies are calculated from the anomaly ${}^{193}m\Delta^{199}$ of the measured A values using the relations ${}^{193}m\Delta_s^{199} = (1.2){}^{193}m\Delta^{199}$, ${}^{193}m\Delta_{1/2}^{199} = (0.2){}^{193}m\Delta^{199}$, and ${}^{193}m\Delta_{3/2}^{199} \approx 0$. We define ${}^{193}m\Delta^{199} = A(193m)g_I(199)/[A(199)g_I(193m)] - 1$.

$a_s(193m)$	- 5696(7) ^b MHz
$a_{1/2}(193m)$	- 812(28) ^b MHz
$a_{3/2}(193m)$	- 70.3(24) ^b MHz
$b_{3/2}(193m)$	10×10^2 MHz

^a C. V. Stager, Phys. Rev. **132**, 275 (1963).

^b Propagated error from the ¹⁹⁹Hg single-electron interaction constants.

Our new data are in satisfactory agreement with the previous level-crossing and optical-spectroscopic results⁵: $A = -2399.63(7)$ MHz and $B = -720(90)$ MHz.

The isotope shifts in optical spectra, for $I \neq 0$, can be determined more precisely with the help of the hfs data obtained from radiofrequency or level-crossing spectroscopy. Thus for ¹⁹³mHg we use the hfs determined in this experiment to re-evaluate the ¹⁹⁶Hg-¹⁹³mHg isotope shift in the 2537-Å line from the measured position of one of the three optical hfs components. The component used, ${}^3P_1(F = \frac{15}{2}) - {}^1S_0$, was the only one which was not overlapped or blended with the lines of other mercury isotopes present in the discharge lamps. The isotope shift (I.S.) is given for two independent optical results in Table IV. These results are discussed in Sec. III C.

C. Discussion

The precise determination of the quadrupole interaction constant of ¹⁹³mHg, in addition to the previously available value of the magnetic interaction constant, allows us to obtain more precise values of the isotope shift and of the quadrupole moment. In particular, the availability of the precisely measured values of A and B allows the use of only the single fully resolved spectral hfs component to determine the isotope shift. Overlap of hfs components of several isotopes produced in the

TABLE IV. ¹⁹³mHg results. The known ¹⁹³mHg nuclear magnetic moment $\mu(193m) = -1.041 658(3) a^{-c} n m$ (without diamagnetic correction) was used in the hfs calculations. For the calculation of the hfs anomaly the g -factor ratio $|g_I(193m)/g_I(199)| = 0.160 940 9(3)$ ^b was used.

A'	-2399.71(3) MHz
B'	-666.5(18) MHz
A	-2399.60(3) MHz
B	-655.6(18) MHz
$\Delta\nu_{15/2-13/2}$	18 569.1(20) MHz
$\Delta\nu_{13/2-11/2}$	14 937.2(22) MHz
${}^{193}m\Delta^{199}$	1.055(1)%
Q	1.2(1) ^d b
¹⁹⁶ Hg- ¹⁹³ mHg I.S.	$369(6) \times 10^{-3} e$ cm ⁻¹
¹⁹⁶ Hg- ¹⁹³ mHg I.S.	$386(8) \times 10^{-3} f$ cm ⁻¹

^a Reference 3.

^b Reference 6.

^c The sign of the magnetic moment is obtained from Refs. 1 and 4.

^d Calculated from B using Q/B given in Ref. 1. The Sternheimer correction is not included.

^e Reference 1. Value recalculated with present hfs data.

^f Reference 4. Value recalculated with present hfs data.

same cyclotron bombardment is frequently a serious problem in optical spectroscopic work. The

essential limitation of the interpretation of the relative isotope and isomer shifts is imposed by the optical spectroscopic measurements. As can be seen from the results given in Table IV, a discrepancy exists in these, pointing to the desirability of independent experiment.

The present work, when complemented by analogous measurements in the ground nuclear state,¹⁹ will allow furthermore a better determination of the isomer shift. This will, in turn, display the deformation dependence of the isomer shift. We recall that in the case of heavy elements the isotope and isomer shifts are determined almost entirely or fully by the variation $\langle R^2 \rangle$ of the nuclear charge distribution. The systematic optical study of the electric and magnetic structure in mercury, which now extends over more than 20 mass numbers when coupled with the recent work of Otten and his co-workers²⁴ on the

short-lived highly-neutron-deficient isotopes, represents the most extensive and detailed one available. For heavier isotopes, it is revealing charge-distribution aspects that exhibit features such as the odd-even staggering in the isotope shifts, which can be correlated with the shell-model nucleon-orbit assignments.¹ For the neutron-deficient ones, on the other hand, a deformed potential, and in particular a sudden jump in deformation when reaching mass 185, has been invoked as a possibility to account for the observations.²⁵

ACKNOWLEDGMENTS

We are grateful to Dr. A. Koehler and the staff of the Harvard University Cyclotron for the irradiations. Some of the computer calculations were performed at the Princeton University Computer Center.

[†]Work supported by the National Science Foundation under Grant No. GP 15258 and in part by the James Arthur Endowment Fund at New York University.

¹W. J. Tomlinson III and H. H. Stroke, *Nucl. Phys.* **60**, 614 (1964).

²O. Redi and H. H. Stroke, *Phys. Rev. A* **2**, 1135 (1970).

³P. A. Moskowitz, C. H. Liu, G. Fulop, and H. H. Stroke, *Phys. Rev. C* **4**, 620 (1971).

⁴S. P. Davis, T. Aung, and H. Kleiman, *Phys. Rev.* **147**, 861 (1966).

⁵W. W. Smith, *Phys. Rev.* **137**, A330 (1965).

⁶R. J. Reimann and M. N. McDermott, *Phys. Rev. C* **7**, 2065 (1973).

⁷A. Bohr and V. F. Weisskopf, *Phys. Rev.* **77**, 94 (1950); H. H. Stroke, R. J. Blin-Stoyle, and V. Jaccarino, *Phys. Rev.* **123**, 1326 (1961).

⁸V. F. Weisskopf, *Ann. Phys.* **9**, 23 (1931); G. Breit, *Rev. Mod. Phys.* **5**, 91 (1933).

⁹F. D. Colegrove, P. A. Franken, R. R. Lewis, and R. H. Sands, *Phys. Rev. Lett.* **3**, 420 (1959); P. A. Franken, *Phys. Rev.* **121**, 508 (1956); for a correction see H. H. Stroke, G. Fulop, S. Klepner, and O. Redi [*Phys. Rev. Lett.* **21**, 61 (1968)].

¹⁰Type PL-40, Polacoat, Blue Ash, Ohio.

¹¹N. Poffé, G. Albouy, M. Gusakov, and J. L. Sarrouy, *J. Phys. Radium* **22**, 639 (1961).

¹²O. Redi and H. H. Stroke (unpublished).

¹³No. 46009, Beckman Instruments, Inc., Fullerton, Cal.

¹⁴In some experiments with nanogram amounts of mercury it has been found that at room temperature all the mercury remains on the walls of the cell, possibly combined chemically with an impurity, and a temperature of at least 100 °C is needed to bring the mercury

into the vapor form.

¹⁵We take into account in calculating R_0 the overlap between the two σ components of ^{198}Hg and absorption lines of $^{193\text{m}}\text{Hg}$.

¹⁶H. Wahlquist, *J. Chem. Phys.* **35**, 1708 (1961).

¹⁷J. P. Barrat, *J. Phys. Radium* **20**, 541 (1959); *J. Phys. Radium* **20**, 633 (1959); *J. Phys. Radium* **20**, 657 (1959).

¹⁸J. Brossel and J. P. Faroux (private communication).

¹⁹G. F. Fulop, C. H. Liu, P. A. Moskowitz, O. Redi, and H. H. Stroke, *Phys. Rev. A* **9**, 593 (1974).

²⁰From the results of Ref. 19, the ^{193}Hg foldover level crossing is expected at a magnetic field $H_c = 7.6^{+1.4}_{-0.3}$ kG. The corresponding magnetic field required for the lamp is sufficiently near that used in this experiment. There was no significant effect caused by the possible overlap of this crossing with those of $^{193\text{m}}\text{Hg}$ on the results.

²¹H. L. Garvin, T. M. Green, E. Lipworth, and W. A. Nierenberg, *Phys. Rev.* **116**, 393 (1959).

²²A. Lurio, M. Mandel, and R. Novick, *Phys. Rev.* **126**, 1758 (1962).

²³The modifications to include the 3P_2 and 3P_0 -state perturbations were made by P. Thaddeus. We have made a further modification to include the perturbations due to the 1P_1 state.

²⁴J. Bonn, G. Huber, H.-J. Kluge, U. Köpf, L. Kugler, E.-W. Otten, and J. Rodriguez, in *Nuclear Moments and Nuclear Structure*, edited by H. Horie and K. Sugimoto [*J. Phys. Soc. Japan* **34** Suppl., 317 (1973)].

²⁵D. Proetel, R. M. Diamond, P. Kienle, J. R. Leigh, K. H. Maier, and F. S. Stephens, *Phys. Rev. Lett.* **31**, 896 (1973).